A plasmodium falciparum sporozoite's journey: through organs and across CD8+ T-cell challenges

Schuijlenburg, R. van

Chapter 6

Intradermal immunization with *Plasmodium berghei* late-arresting genetically attenuated sporozoites induces PD-L1 expression on regulatory macrophages and dendritic cells

Roos van Schuijlenburg, Chanel M. Naar, Helena M. de Bes-Roeleveld, Séverine Chevalley-Maurel, Lili A. Zigó, Emma L. Houlder, Joost M. Lambooij, Els Baalbergen, Meta Roestenberg, Blandine Franke-Fayard

Scientific reports, 2025. DOI: 10.1038/s41598-025-27588-4


Intravenous
Intradermal

Abstract

The development of effective and long-lasting malaria vaccines remains a key goal. Late-arresting genetically attenuated sporozoite (LA-GAP SPZ) vaccines, such as PfΔmei2 (GA2), have shown strong protective potential. While GA2 delivered via mosquito bites has demonstrated up to 90% protection in humans, practical vaccine deployment will require alternative administration routes. Intravenous (IV) delivery of whole SPZ vaccines has been highly effective, but intradermal (ID) administration though easier, offers significantly reduced protection, with unclear underlying mechanisms.

In this study, we used a *Plasmodium berghei* GA2 SPZ rodent model to compare immune responses following ID and IV immunization across multiple organs. ID immunization resulted in lower frequencies of $CD8^+$ tissue-resident memory T cells (Trm) in the spleen (1.3%, $p = 0.3$), lungs (8.1%, $p = 0.005$) and liver (2.5%, $p = 0.07$), along with reduced activation markers (Granzyme A, Ki67, and KLRG1). In the liver, Granzyme B ($p = <0.0001$) and perforin ($p = <0.0001$) were significantly decreased after ID immunization, indicating diminished cytotoxic potential. Importantly, ID immunization induced a regulatory myeloid phenotype in the skin and skin-draining lymph nodes, marked by low CD86 and high PD-L1 expression, potentially impairing T cell priming. A similar regulatory profile in the liver suggests systemic immunosuppression.

These findings highlight key immunological differences between ID and IV GA2 SPZ delivery and suggest that optimizing ID administration, such as adjusting injection volume to enhance sporozoite migration, may improve efficacy. Understanding how myeloid regulation and T-cell activation vary across organs is essential for enhancing malaria vaccine strategies.

Introduction

The approval of two groundbreaking malaria vaccines, RTS,S and R21, which are based on the circumsporozoite protein (CSP) found on the surface of sporozoites (SPZ, the infective form of malaria) marks a significant milestone in malaria vaccine research (WHO). However, to eliminate malaria, vaccines with higher efficacy and durability are desperately needed. Late-arresting genetically attenuated SPZ vaccination (LA-GAP) presents a promising solution by inducing both cellular immune responses and CSP-targeting antibodies, resulting in high-level protection even after a single immunization in malaria-naïve individuals [1]. This LA-GAP vaccine, known as PfΔmei2 (GA2), lacks the mei2-like RNA gene, allowing sporozoites to travel through the bloodstream, infect hepatocytes and develop into liver schizonts similar to wild-type SPZ [2]. However, during the late liver stage, the GA2 liver schizont arrests its development, in contrast to the wild-type liver schizont, which bursts and releases merozoites that infect red blood cells [3, 4]. Previous comparisons between early (GA1) and late (GA2) genetically arresting parasites in humans have demonstrated that development until the late liver stage is essential for achieving high-level protection [5]. Moreover, this protection was associated with T cell activation in peripheral blood mononuclear cells of these individuals, particularly $CD4^+$ pluripotent T-cells producing multiple Th1-type cytokines [1, 5].

Whereas in these human trials $CD8^+$ T cell activation could not be detected in the peripheral blood circulation, animal models have shown that liver tissue-resident $CD8^+$ T cells ($CD8^+$ Trm cells) are associated with protection from liver-stage malaria [6-8]. It is thought that these cells cannot be detected in the peripheral circulation due to their low frequency, whereas they are increased in livers of protected animals. It is hypothesized that $CD8^+$ Trm cells can recognize and kill malaria-infected hepatocytes, as indicated by their increased expression of granzyme B, perforin, and the cytokine IFNγ [9, 10]. However, these liver $CD8^+$ Trm cells require priming before they can specifically recognize and kill malaria-infected hepatocytes [11, 12]. Naïve $CD8^+$ T cells can be primed in secondary lymphoid organs by antigen-presenting cells (APC) like macrophages and dendritic cells [13-15]. After priming, naïve $CD8^+$ T cells differentiate into $CD8^+$ Trm cells and migrate to the liver [6, 7, 16]. Priming of naïve $CD8^+$ T cells can occur in different organs before SPZ infect hepatocytes [9].

After a single mosquito bite, roughly 100 SPZ are deposited in the skin [17], where antigens can be processed by APC such as macrophages and dendritic cells. Subsequently, around 15-20% of SPZ migrate to the skin-draining lymph node (skin dLN)

while ± 20% enter the bloodstream [17-19], traveling through the lungs and spleen before reaching the liver to infect hepatocytes [20]. In the meantime, skin-resident dendritic cells that have encountered SPZ process the antigens and migrate to the skin dLN [14]. Previous studies have demonstrated that through these routes $CD8^+$ T cells, can be primed by APC in the skin dLN and migrate to the liver [11, 13, 21].
Although the administration of GA2 SPZ in humans through mosquito bites has proven effective [1, 5], alternative routes of administration will be required to develop this concept into a vaccine. Interestingly, for other whole SPZ vaccines such as the irradiated SPZ, it has been shown that intradermal (ID) administration results in much lower protection compared to intravenous (IV) administration in humans [22, 23]. This reduced efficacy was initially thought to be related to the number of SPZ entering the liver. Using rodent bioluminescent parasites in animal models, it was indeed shown that IV-injected SPZ reach the liver more efficiently as compared to the ID-administered SPZ. However, when we corrected for the lower parasitic liver load by increasing the ID-administered parasites 5-fold, we found that GA2 *Plasmodium yoelii* (*Py*) SPZ immunized mice are after ID administration less protected as compared to IV administration [24]. The mechanism behind this observation remained unclear. These findings suggest that the altered biodistribution of SPZ after ID administration in organs other than the liver negatively impacts protective responses in the liver. Therefore, we aimed to investigate whether GA2 SPZ following ID or IV administration in organs other than the liver could negatively impact T-cell responses in the liver.

Methods

Mosquito production

Mosquitoes from a colony of *Anopheles stephensi* (line Nijmegen SDA500) were used to obtain sporozoites. Larval stages were reared in water trays at a temperature of 28 ± 1°C and a relative humidity of 80%. Adult females were transferred to incubators with a temperature of 26 ± 0.2°C and a relative humidity of 80%. For all the experiments, 3- to 5-day-old mosquitoes were used. The *Plasmodium berghei* (Pb) infected mosquitoes were maintained at 21°C at 80% relative humidity.

Experimental animals, *P. berghei* parasite line

Female OF1 mice and female and male C57BL/6J mice (Charles River Laboratories, France) of 4-6 weeks old were acclimatized for one week prior to the experiment. Mice were housed between 4-5 mice per cage in ventilated cages with autoclaved aspen woodchip, fun tunnel, wood chew block and nestlets (12:12 hour light-dark cycle; 21 ± 2°C; relative humidity of 55 ± 10%). During the experiment mice were fed with

commercially prepared autoclaved dry rodent diet pellets and water, both available ad libitum. All animal experiments were approved with license 11600202216547 by the Competent Authority after advice on ethical evaluation by the Animal Experiments Committee Leiden and were performed in accordance with the Experiments on Animals Act (Wod, 2014) the applicable legislation in the Netherlands in accordance with the European guidelines (EU directive no 2010/63/EU). The study was executed in a licensed establishment for experimental animals, and conducted in accordance with the ARRIVE guidelines.

Humane endpoints: the animals/body condition was thoroughly examined daily. Animals were humanely sacrificed in case the following defined endpoints are reached: visible pain (abnormal posture and/or movement), abnormal behaviour (isolation, abnormal reaction to stimuli, no food and water intake). If distress of the animals was observed by the animal caretakers, this was reported to the investigators and according to the therefore mentioned criteria, the animals were taken out of the experiment and euthanized. In all experiments no mice were euthanized before termination of the experiment and no mice died before meeting criteria for euthanasia.

The LA-GAP PbΔmei2Δlisp2 parasite (2900cl3, mutant RMgm-4937; www.pberghei.eu), which is genetically attenuated by the deletion of the meiosis inhibited 2 (mei2) and liver-specific protein 2 (lisp2) genes was used [2]. Feeding of *Anopheles stephensi* mosquitoes was performed as described previously [42].

***In vivo* immunization of mice with *Pb* SPZ**

The study including data acquisition was performed blinded. The study was deblinded after analysis of the data.

One day prior to immunizations, mice were randomly divided into three or four different groups (4-5 mice per group, maximum of 20 mice per experiment). On the day of immunizations, salivary glands (21-23 days post blood meal) of *P. berghei* LA-GAP Pb*Δmei2Δlisp2* (*Pb* GA2 SPZ) infected mosquitoes were dissected in cold RPMI 1640 glutamax (Thermo Fisher). As a control, salivary glands from the same batch of uninfected mosquitoes, hence referred to as salivary gland extract (SGE), were dissected in cold RPMI 1640 glutamax (Thermo Fisher). Immediately after dissection the glands were crushed and homogenized and the total number of *Pb* GA2 SPZ was counted. Intravenous immunization in the tail vein was performed after warming the mice under a heath lamp set at 35°C to dilate the veins. For intravenous immunization, 25,000 *Pb* GA2 SPZ were inoculated in 200 µL RPMI 1640 glutamax (Thermo Fisher). For

intradermal immunizations, the mice were anesthetized with isoflurane and 125,000 live *Pb* GA2 SPZ were inoculated in 20 µL RPMI 1640 glutamax (Thermo Fisher) in the left shaved upper thigh. For the SGE control, an equal amount of SGE was injected in 200 µL IV or 20 µL ID RPMI 1640 glutamax (Thermo Fisher) and for the medium control, 200 µL IV or 20 µL ID RPMI 1640 glutamax (Thermo Fisher). Second immunizations were given 7 days after the first. All injections were given between 1 pm and 3 pm (methods Figure 6).

Determination of parasite liver load after 1st and 2nd immunization by real-time *in vivo* imaging

After 44 hours post-immunization the parasitic liver load was determined through bioluminescent imaging. Imaging was performed using the IVIS Lumina II Imaging System (Perkin Elmer Life Sciences, Waltham, USA) [43] 8 minutes after a subcutaneous injection with D-luciferin dissolved in PBS (100 mg/kg; Caliper Life Sciences, USA). Quantitative analysis of the bioluminescence of whole bodies was performed by measuring the luminescence signal intensity using the ROI (region of interest) settings of the Living Image® 4.4 software. Blood-stage breakthroughs were checked at 5-6 days post 1st immunization and 2nd immunization. If any parasites were discovered in the blood the mice were sacrificed and eliminated from the experiment (methods Figure 6).

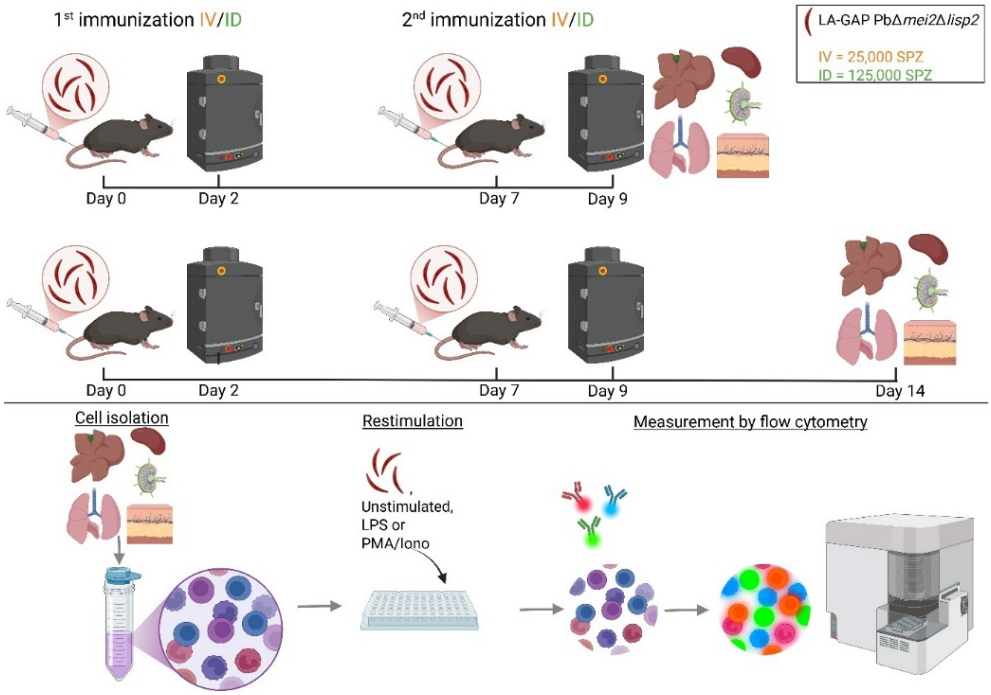

Methods Figure 6. Experimental set-up. Overview of the timeline of mice immunizations via IV or ID. 2 days after immunizations, the parasitic liver-load was determined by IVIS. For the early immune response (myeloid activation), organs were harvested 2 days post 2nd immunization ID/IV. For the late immune response (T cell activation), cells where organs were harvested 7 days post 2nd immunization ID/IV. Cells were isolated from the organs and restimulated with GA2 SPZ, LPS, PMA/Iono or unstimulated. After 4 hours of incubation, cells were stained with fluorescent antibodies and measured by flow cytometry.

Organ harvesting and processing

Two days or seven days after the final immunizations, mice were anesthetized via intraperitoneal injection of 10% ketamine (Dechra Pharamceuticals, Northwich, UK) with 20 mg/mL xylazine (Alfasan, Woerden, The Netherlands). Blood was collected via retro-orbital puncture using a glass capillary tube and transferred into 1.5 mL Eppendorf tubes pre-coated with heparin, and put on ice. The blood was spun down at 4°C, plasma was collected and stored at -80°C. The liver and lungs were perfused by slowly injecting 20 mL cold PBS via the heart, followed by dissection of the liver, lungs and spleen after IV immunizations, and liver, lungs, spleen, skin and skin dLN after ID immunizations, and placed in sterile RPMI 1640 glutamax (Thermo Fisher) on ice. The mice were killed by exsanguination.

Livers were processed via mincing with a blade and placed in a 50 mL tube with 20 mL RPMI 1640 glutamax containing 1 mg/mL Collagenase IV (Sigma-Aldrich) and 2,000 U/mL DNase I (Sigma-Aldrich) and incubated for 45 minutes at 37°C, mixing once during incubation. After incubation, tubes were placed on ice and poured through a 100-micron filter (BD) and washed with 20 mL PBS supplemented with 1% Fetal Calf Serum (FCS) and 2.5 mM ethylenediamine tetra-acetic acid (EDTA, Sigma-Aldrich). The tubes were spun down at 1,500 rpm for 10 minutes at 4°C and supernatants were gently taken off, after which PBS supplemented with 1% FCS and 2.5 mM EDTA was added to the pellets and tubes were spun down at 50 g for 3 minutes at 4°C. To separate the immune cells from the hepatocytes, the supernatant, which contains immune cells, was gently removed. The immune cells were spun down for 10 minutes at 1,600 rpm at 4°C. The supernatant was discarded, and 3 mL sterile PBS supplemented with 0.15M NH_4Cl; 1mM $KHCO_3$; 0.1 mM Na_2EDTA was added for 2 minutes to lyse red blood cells, followed by the addition of 7 mL PBS supplemented with 1% FCS and 2.5 mM EDTA (Sigma-Aldrich). The tubes were spun down for 10 minutes at 1,600 rpm at 4°C. The supernatant was discarded, and the pellet was resuspended in 10 mL PBS supplemented with 0.5% bovine serum albumin (Fraction V, Roche) and 10 mM ETDA (Sigma-Aldrich) and spun down for 10 minutes at 1,200 rpm at 4°C. The supernatant was removed, and 35 µL CD45 MicroBeads (Miltenyi Biotec) were added and incubated for 15 minutes in the fridge. After incubation, the left-over beads were washed off by adding 10 mL PBS supplemented with 0.5% bovine serum albumin (Fraction V, Roche) and 10 mM ETDA and spun down for 10 minutes at 1,600 rpm at 4°C. The pellets were resuspended in 5 mL PBS supplemented with 0.5% BSA (Fraction V, Roche) and 10 mM ETDA and run through a pre-wetted LS magnetic column according to protocol (Miltenyi Biotec). The columns were washed with RPMI 1640 glutamax, 5% FCS, 0.1% β-mercaptoethanol, 100U/mL penicillin, and 100 µg/mL streptomycin (culture medium) to collect the $CD45^+$ cells. The tubes were spun down for 10 minutes at 1,600 rpm at 4°C, supernatants were taken off and resuspended in 5 mL washing medium, and viable cells were counted using trypan blue and a Bürker counting chamber.

To process lungs, the lungs were chopped into small pieces using a scalpel and transferred to a 15-mL tube. To digest the tissue 5 mL RPMI 1640 glutamax supplemented with 1 mg/mL Collagenase IV (Sigma-Aldrich), 2 µL/mL DNase (Sigma-Aldrich), and 2 µL/mL of 1M $CaCL_2$ (Sigma-Aldrich) and incubated for 30 minutes at 37°C. After incubation, 10 mL cold RPMI 1640 glutamax with 5% FCS was added and poured through a 100-micron filter (BD). A 1 mL syringe was used to mash the digested tissue and washed with 20 mL cold RPMI 1640 glutamax with 5% FCS. The tubes were

spun down for 10 minutes at 1,600 rpm at 4°C, and 2 mL sterile PBS supplemented with 0.15M NH_4Cl; 1mM $KHCO_3$; 0.1 mM Na_2EDTA was added for 2 minutes to lyse the red blood cells. After 2 minutes 8 mL of washing medium was added, and tubes were spun down for 10 minutes at 1,600 rpm at 4°C. Pellets were resuspended in 5 mL of washing medium, and viable cells were counted using trypan blue and a Bürker counting chamber.

To process the spleen and skin-draining lymph nodes, the organs were crushed with the back of a syringe. A two-fold concentrated enzyme mix in RPMI was added, end concentration of 1 mg/mL Collagenase D (Roche) and 2000 U/mL DNase (Sigma), was added and samples were incubated for 20 minutes at 37°C. After incubation, the cells were poured through a 100-micron filter (BD) and washed with 10 mL cold RPMI medium. The cells were spun down for 10 minutes at 1600 rpm at 4°C. The supernatant was discarded, and 2 mL cold sterile PBS supplemented with 0.15M NH_4Cl; 1mM $KHCO_3$; 0.1 mM Na_2EDTA was added for 2 minutes to lyse red blood cells. Lysis was stopped by the addition of 8 mL cold RPMI, and the pellet was resuspended in 10-20 mL cold RPMI 1640 glutamax (Thermo fisher) supplemented with 100U/mL penicillin and 100 µg/mL streptomycin (Sigma-Aldrich), 0,1 % β-mercaptoethanol, and 5% FCS and counted using trypan blue and a Bürker counting chamber.

To process the skin, the skin was cut into small pieces and incubated with enzymes P, D and A, diluted in buffer L according to the manufacturer's instructions for the whole skin dissociation kit (Miltenyi). Samples were incubated for 3 hours at 37°C. After incubation, 500 µL of cold RPMI 1640 glutamax (Thermo fisher) supplemented with 100U/mL penicillin and 100 µg/mL streptomycin (Sigma-Aldrich) and 5% FCS was added. The tubes were spun according to the tumor program with the MACS dissociator (Miltenyi) and centrifuged for 10 minutes at 1200 rpm at 4°C. The cells were poured through a 100-micron filter (BD) and washed with 10 mL cold RPMI medium. The cells were spun down for 10 minutes at 1200 rpm at 4°C, and the pellet was resuspended in 1 mL cold RPMI 1640 glutamax (Thermo fisher) supplemented with 100U/mL penicillin and 100 µg/mL streptomycin (Sigma-Aldrich), 0,1 % β-mercaptoethanol, and 5% FCS. Cell counts and viability were assessed using trypan blue exclusion and a Bürker counting chamber.

Cell stimulation and analysis

A total of 200,000 cells per well were added. For specific restimulation, live *Plasmodium berghei* GA2 SPZ in a concentration of 25,000/mL (5,000 per 200,000 cells) in culture

medium: RPMI 1640 glutamax (Thermo fisher) supplemented with 100U/mL penicillin and 100 µg/mL streptomycin (Sigma-Aldrich), 0,1 % β-mercaptoethanol and 5% FCS, were added to each well and spun down for 4 minutes at 1,200 rpm at 4°C. For the specific restimulation, 0.1 µg/mL Phorbol 12-myristate 13-acetate (PMA) + 1 µg/mL ionomycin (Iono) (Sigma-Aldrich) in culture medium was added. To measure intracellular cytokine expression, 10 µg/mL Brefeldin A (Sigma-Aldrich) was directly added. All plates for flow cytometry were incubated for 4 hours at 37°C with 5% CO_2.

After 4 hours (flow cytometry measurement), the cells were transferred into a V-bottom plate and washed with cold PBS. Cells were stained with live/dead marker Zombie NIR (Thermo Fisher), fixed with eBioscience FOXP3/Transcription Factor Fixation/Permeabilization kit, and stained with different markers for 3 different panels: (1) Myeloid panel (Table 1), (2) T-cell panel (Table 2), or (3) Advanced T-cell panel (Table 3, implemented halfway through the experiments). To all panels, Fc-block (BD bioscience), True-Stain Monocyte Blocker (BioLegend), and Brilliant Violet buffer (Thermo Fisher) was added. The cells were measured by flow cytometry using Aurora 5 laser (Cytek Bioscience B.V., Amsterdam) and analyzed using Spectroflow (Cytek Bioscience B.V.), FlowJo version 10.8 (FlowJo LLC), and R-studio version 1.4.1717. For gating strategy see supplementary figure 2. Of the $CD4^+$ and $CD8^+$ T-cells were gated into effector memory T cells (Tem, $CD44^{hi}$ $CD62L^-$ $CD69^-$), resident memory -cells (Trm, $CD44^{hi}$ $CD62L^-$ $CD69^+$) and DN cells into DN1, DN2, DN3 and DN4 based on expression of CD44 and CD25 expression.

Table 1. Myeloid panel

Target	Antibody clone	Fluorochrome
MHCII	2G9	BUV395
PD-L1	B7-H1	BUV737
CD11c	N418	BV421
Siglec F	E50-2440	BV480
CD40	3-23	BV510
CCR7	4B12	BV605
XCR1	ZET	BV650
F4/80	T45-2342	BV711
CD45	30-f11	BV785
CD70	FR70	FITC
Ly6C	HK1.4	Percp-cy5.5
CD80	16-10A1	PE

CD64	X54-5/7.1	PE-Dazzle
B220	RA3-6B2	PE-Cy5
CD11b	M1/70	PE-Cy7
CD206	C068C2	APC
TIM4	F31-5G3	AF647
CD86	GL1	AF700
NK1.1	PK135	APC-Cy7

Table 2. T-cell panel

Target	Antibody clone	Fluorochrome
CD3	17A2	BUV661
CD45	30-F11	BUV805
CXCR3	CXCR3-173	Super Bright 436
Ki67	SolA15	eFluor 506
γδ T-cells	GL3	BV605
CD4	GK1.5	BV650
PD-L1	10F.9G2	BV711
PD1	29f.1A12	BV785
Perforin	eBio0mak	FITC
CD44	1M7	AF532
CD8	53-6.7	PerCP
Granzyme A	GrA-368.5	PerCP-ef710
CD137	4-1BB	PE
CD69	H1.2F3	PE-cf594
IFNγ	XMG1.2	PE-Cy5
KLRG1	2F1	PE-Cy5.5
TNFα	MPG-XT22	PE-Cy7
FOXP3	FjK-16s	APC
Granzyme B	NGZB	efluor 660
CD25	PC61.5	AF700

Table 3. Advanced T-cell panel

Target	Antibody clone	Fluorochrome
MHCII	2G9	BUV395
CD25	PC 61.5	BUV563
CD3	17A2	BUV661
CD62L	Mel-14	BUV737

CD45	30-f11	BUV805
CXCR3	CXCR3-173	Super bright 436
γδ T-cells	GL3	BV605
CD4	GK1.5	BV650
CD11c	N418	BV711
PD1	29f.1A12	BV785
CD40L	SA047C3	FITC
CD44	IM7	AF532
CD8	53-6.7	PerCP
CD64	X54-5/7.1	PerCP-efluor 710
CD69	H1.2F3	PE-cf594
IFNγ	XMG1.2	PE-Cy5
KLRG1	2F1	PE-Cy5.5
TNFα	MPG-XT22	PE-Cy7
CD86	GL1	AF700
NK1.1	PK135	APC-Cy7

Statistical analysis

Data was analysed using Spectroflow (Cytek Bioscience B.V., Amsterdam) and FlowJo version 10.8 (FlowJo LLC, Ashland, OR, USA), R studio version 4.3.1 and Adobe Illustrator 2023. Sample size estimation was performed with a power analysis using an alpha of 0.05 and a power of 90%. Statistical analyses were performed using one-way ANOVA with multiple comparisons with Bonferroni correction or an independent t-test with R studio version 4.3.1. Significance was defined as a p-value of less than 0.05. Data subjected to parametric statistical analyses had its normality confirmed beforehand.

Results

Distribution of immune cells in the spleen, lung and liver after intradermal or intravenous sporozoite GA2 immunization

First, we observed the parasitic liver load after IV or ID immunization. Here we found a negative parasitic liver load after the 2nd IV GA2 SPZ immunization but a comparable parasitic liver load between the 1st and 2nd ID GA2 SPZ immunization (Sup Fig. 1). To compare the immune response after ID immunization or IV immunization with GA2 SPZ, we analyzed shifts in the number of immune cells in the spleen, lung and liver two days after the 2nd and last immunization. Here, we observed that IV GA2 SPZ immunization leads to marked increases in total numbers of immune cells in the liver, and small increases in the spleen but no changes in the lungs (Fig. 1A). After ID immunization,

these increases were not detected, resulting in a statistically significant lower number of cells in the ID vs IV condition in the liver (p = 0.0003). Furthermore, only in the liver after IV immunization did we observe a significant difference between SGE and LA-GAP (p = <0.0001, Fig 1A). This is in line with the absolute number of various immune cell populations, where we primarily observe a significant increase in the liver following IV immunization compared to ID immunization (Sup Fig. 3). Next, after identifying immune cell subsets by antibody staining and flow cytometry, we investigated the overall kinetics of immune cell distribution in the spleen, lungs and liver after ID versus IV GA2 SPZ immunization. Looking at cell immune subsets 2 days after the 2nd immunization, we observed slightly lower total numbers of γδ T cells (5.5%, p = 0.05) and CD3$^+$ T cells (8.5%, p = 0.0003) in the lungs and CD3$^+$ T cells in the liver (9.3%, p = 0.0001) after ID GA2 SPZ immunization compared with IV GA2 SPZ immunization (Fig. 1B). However, 7 days after the 2nd immunization of the total number of CD3$^+$ T cells, the CD4$^+$ (2.2%, p = 0.01) and double negative (DN) T cells (3.2%, p = 0.04) in the spleen, and DN (7.4%, p = 0.01) and CD8$^+$ T cells (6.1%, p = 0.06) in the lungs were most affected with a lower number after ID GA2 SPZ immunization compared with IV GA2 SPZ immunization. In contrast, these differences were not observed in the liver. Interestingly, CD4$^+$ T cells in the lungs exhibited the opposite trend, showing an increase after ID immunization (8.4%, p = 0.02, Fig. 1C). Last, we focused on the differentiation markers within different lineages, e.g. within the CD4$^+$, CD8$^+$ and DN T cells 7 days after the 2nd GA2 SPZ immunization. Here we observed a lower percentage of CD4$^+$ Trm in the spleen (4.2%, p = 0.01), lungs (10.7%, p = 0.0006) and liver (4.2%, p = 0.2) after ID GA2 SPZ immunization compared with IV GA2 SPZ immunization (Fig. 1D). For the CD4$^+$ Tem we also found lower numbers in the liver (3.3%, p = 0.06) after ID immunization compared with IV immunization, but not in the spleen and lungs (Fig. 1D). For the CD8$^+$ T cells we similarly observed a lower percentage Trm in the spleen (1.3%, p = 0.3), lungs (8.1%, p = 0.005) and liver (2.5%, p = 0.07) and also Tem in the spleen (27.3%, p = 0.006), lungs (13.2%, p = 0.002) and liver (19.6%, p = 0.0001) after ID GA2 SPZ immunization compared with IV GA2 SPZ immunization (Fig. 1E). Interestingly, for the DN T cells we found a higher percentage of DN1 T cells in the spleen (13%, p =0.004), lungs (12%, p = 0.01) and liver (16%, p = 0.01) after ID GA2 SPZ immunization compared with IV GA2 SPZ immunization (Fig. 1F). This indicates that the differentiation of DN T cells after ID SPZ immunization is less progressed at 7 days after 2nd immunization compared with IV SPZ immunization. Overall, these findings show a lower amount of γδ T cells, CD3$^+$ T cells, CD4$^+$ Tem , CD8$^+$ Tem and Trm and more DN1 T cells after ID SPZ immunization compared with IV SPZ immunization in the spleen, lungs and liver.

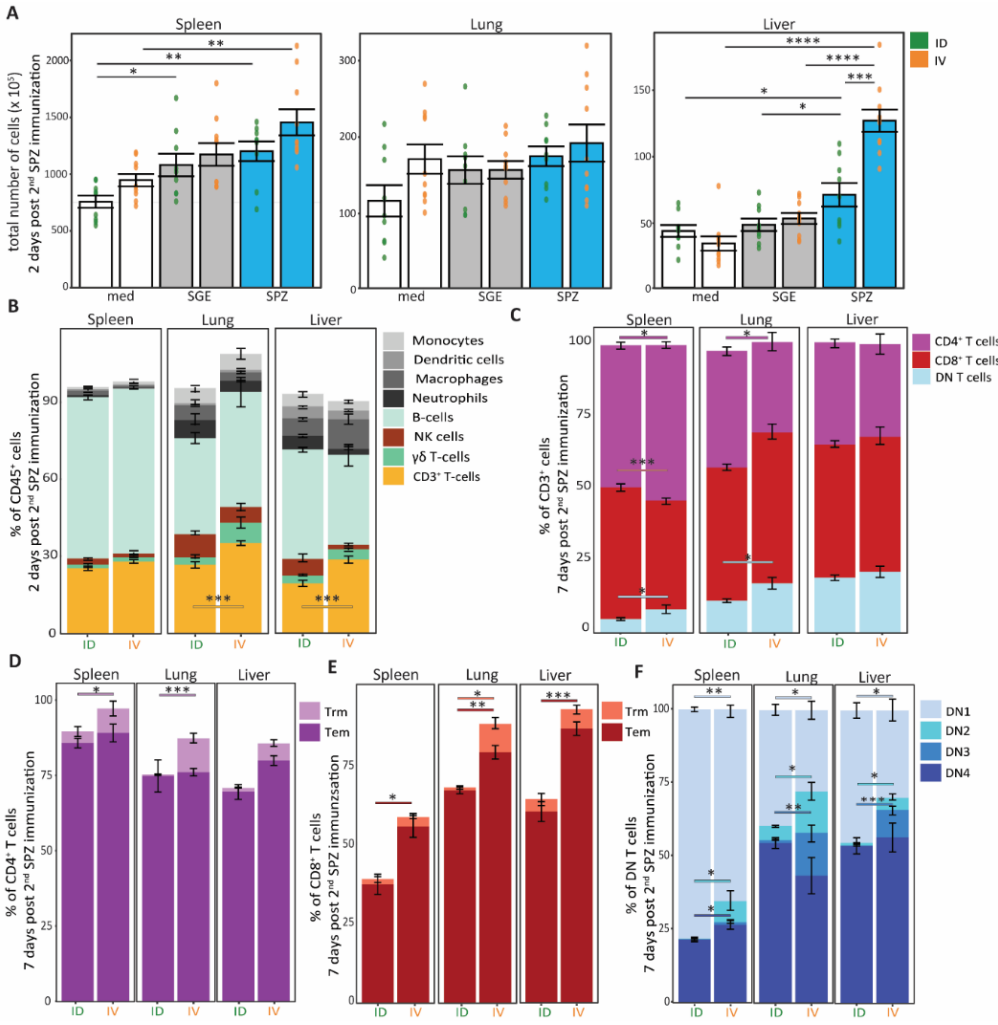

Figure 1. Distribution of immune cells in the spleen, lungs and liver after intradermal (ID) or intravenous (IV) SPZ GA2 immunization. (**A**) Total number of immune cells in the spleen, lungs or liver, 2 days after 2nd ID (green) or IV (orange) immunization *ex vivo* with medium (white), salivary gland extract (SGE) (grey) or SPZ (blue). (**B**) Kinetics of immune cells in the spleen, lungs and liver 2 days after 2nd SPZ ID or IV immunization followed by *in vitro* restimulation with LA-GAP SPZ. (**C**) $CD3^+$ T cell distribution in the spleen, lungs and liver, 7 days after 2nd SPZ ID or IV immunization followed by *in vitro* restimulation with LA-GAP SPZ. (**D**) Distribution of Trm and Tem $CD4^+$ T cells in the spleen, lungs and liver, 7 days after 2nd SPZ ID or IV immunization. (**E**) Distribution of tissue-resident memory (Trm) and effector memory (Tem) $CD8^+$ T cells in the spleen, lungs and liver, 7 days after 2nd SPZ ID or IV immunization followed by *in vitro* restimulation with LA-GAP SPZ. (**F**) Distribution of double negative 1 (DN1), DN2, DN3 and DN4 T cells in the spleen, lungs and liver, 7 days after 2nd

SPZ ID or IV immunization followed by *in vitro* restimulation with LA-GAP SPZ. ID immunization n=9 per group, IV immunization n=10 per group divided over 2 independent experiments. Statistical significance between groups was assessed by one-way ANOVA with multiple comparisons or an independent t-test. *p<0.05, **p<0.005, ***p<0.0005, and ****p<0.0001.

Activation of T cells in the spleen, lungs and liver after intravenous or intradermal GA2 SPZ immunization

Having found a difference in $CD4^+$ Tem, $CD8^+$ Tem and Trm and DN1 T cells after ID immunization, we next investigated the activation of T cells in the spleen, lungs and liver after ID and IV immunization at the later timepoint: 7 days post 2nd GA2 SPZ immunization. An optimized t-Ditributed Stochastic Neighbor Embedding (opt-SNE) analysis based on different T cell markers revealed activation of two cell clusters after IV GA2 SPZ immunization, which were not activated after ID GA2 SPZ immunization. We identified that these clusters consisted of $CD8^+$ T cells and DN T cells which highly expressed Granzyme A, Ki67 and KLRG1 (Fig. 2A+B+C). Therefore, we analyzed the percentage of Granzyme A^+, $Ki67^+$ and $KLRG1^+$ $CD8^+$ T cells and DN T cells. Here we observed an overall lower percentage of expression on DN T cells after ID GA2 SPZ immunization compared with IV GA2 SPZ immunization in markers for Granzyme A^+ (spleen 6.1%, lung 19.3%, liver 13.8%), $Ki67^+$ (spleen 5.6%, lung 8.8%, liver 11.6%) and $KLRG1^+$ (spleen 6.3%, lung 13.6%, liver 8.9%) $CD8^+$ T cells and Granzyme A^+ (spleen 11.9%, lung 26%, liver 20.1%), $Ki67^+$ (spleen 2.4%, lung 8.6%, liver 15.2%) and $KLRG1^+$ (spleen 9.1%, lung 12.9%, liver 12.4%) respectively. Interestingly, after SGE immunization, we observed minimal differences in the percentages of Granzyme A^+, $Ki67^+$ and $KLRG1^+$ $CD8^+$ T cells and DN T cells between ID and IV immunization, which indicates that the immune differences are GA2 SPZ specific (Fig. 2D+E). In parallel, γδ T cells exhibited significantly lower expression of Ki67 ($p = 0.02$) and KLRG1 ($p = 0.04$) in the lungs as well as a reduced Ki67 expression in the liver ($p = 0.02$) after ID GA2 SPZ immunization compared with IV (Sup Fig. 4B), indicating that these cells are phenotypically also less activated after ID immunization. To further investigate the killing pathway of T cells we looked into the expression of Granzyme B and perforin. In the spleen, no differences were observed between ID and IV GA2 SPZ immunization. However, in the lung expression of Granzyme B on both $CD8^+$ T cells ($p = 0.0003$) and DN T cells ($p = 0.07$) and in the liver expression of both Granzyme B and perforin on $CD8^+$ T cells ($p = <0.0001$, $p = <0.0001$) and DN T cells ($p = 0.06$, $p = <0.0001$) was lower after ID GA2 SPZ immunization compared with IV GA2 SPZ immunization (Fig. 2F). This is in line with the decreased expression of Granzyme B on $CD4^+$ T cells in the liver after

ID immunization compared with IV immunization (p = 0.001, Sup Fig. 4A). Last, we investigated the expression of cytokines IFNγ and TNF on $CD8^+$ T cells and DN T cells. Here we did not observe any differences in cytokine expression between ID and IV GA2 SPZ immunization in any of the organs (Fig. 2G).

In conclusion, ID GA2 SPZ immunization compared to IV delivery results in suppressed activation of the $CD8^+$ T cell and DN T cell compartments, primarily in the lungs and liver, visible by the number of Granzyme A^+, $Ki67^+$ and $KLRG1^+$ $CD8^+$ T cells and DN T cells. Furthermore, in the liver, ID GA2 SPZ immunization leads to decreased perforin and Granzyme B expression compared to IV GA2 SPZ immunization.

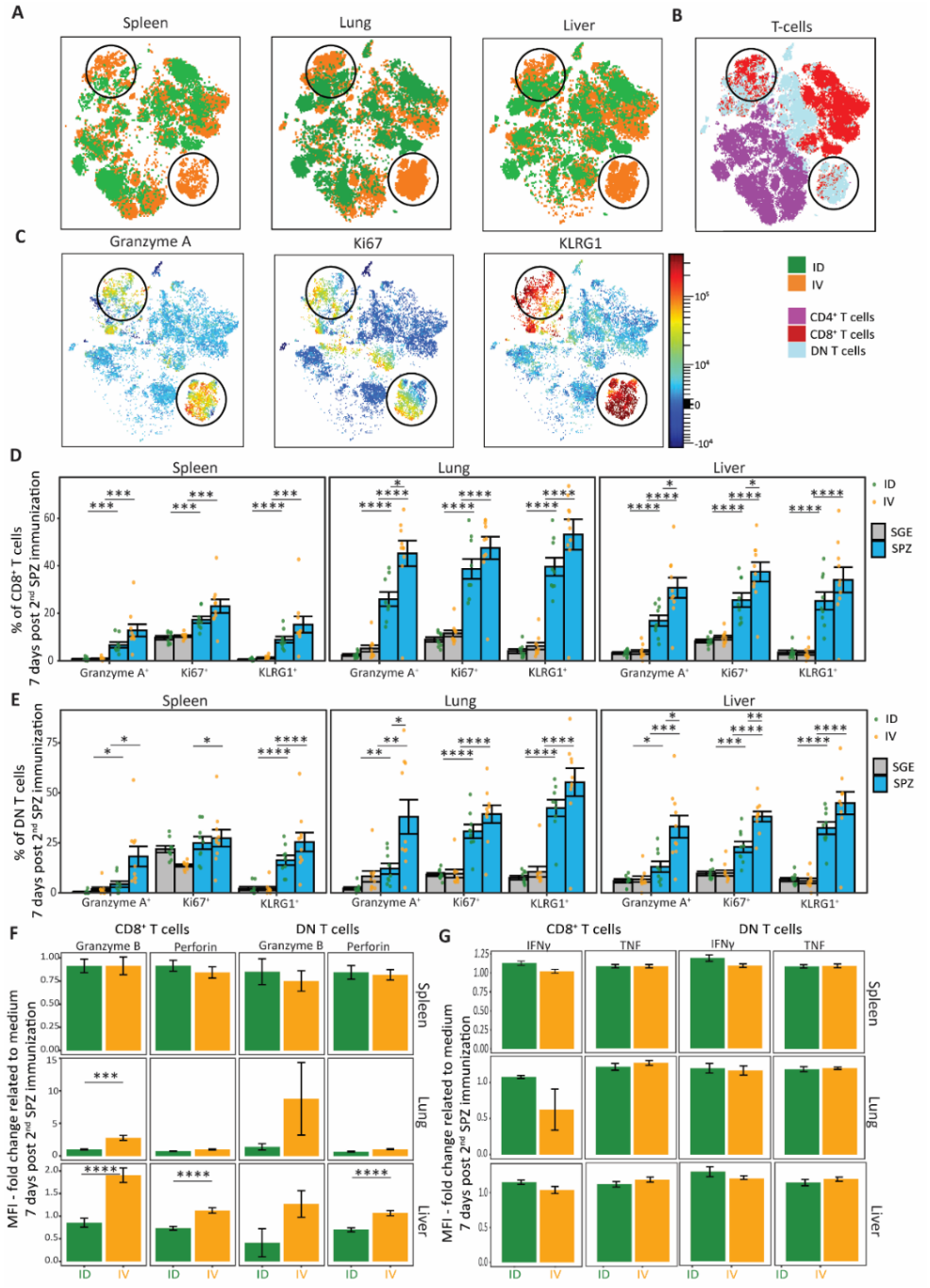

Figure 2. T cell activation in the spleen, lung and liver after intradermal (ID) or intravenous (IV) GA2 immunization. **(A)** Opt-SNE of different activation markers on T cells after ID

(green) or IV (orange) immunization in the spleen, lung and liver. (**B)** Identification of $CD4^+$ (purple), $CD8^+$ (red) and DN T cells (light blue) in the opt-SNE. (**C)** Expression of Granzyme A, Ki67 and KLRG1 in the opt-SNE. (**D + E)** Percentage of Granzyme A^+, $Ki67^+$ and $KLRG1^+$ $CD8^+$ (**D**) or DN T cells (**E**) in the spleen, lung and liver after SGE (grey) or GA2 SPZ (blue) ID (green dots) or IV (orange dots) immunization. (**F + G)** Fold change relative to medium expression of Granzyme B, Perforin (**F**) and IFNγ and TNF (**G**) on $CD8^+$ T cells and DN T cells in the spleen, lung and liver. ID GA2 SPZ immunization in green, IV GA2 SPZ immunization in orange. ID immunization n=9 per group, IV immunization n=10 per group divided over 2 independent experiments. All conditions were *in vitro* restimulated with LA-GAP SPZ. Statistical significance between groups was assessed by one-way ANOVA with multiple comparisons or an independent t-test. *p<0.05, **p<0.005, ***p<0.0005, and ****p<0.0001.

Activation of myeloid cells in the spleen, lungs and liver after intravenous or intradermal GA2 SPZ immunization

To investigate the underlying mechanism behind the reduced number of activated T cells after ID GA2 SPZ immunization, we analyzed the impact of ID GA2 SPZ immunization on the activation of myeloid cells in the spleen, lungs and liver compared with IV GA2 SPZ immunization at the early timepoint 2 days post 2^{nd} immunization. Principal Component Analysis (PCA) revealed distinct immunological profiles between the two routes of administration across the spleen, lungs and liver (Fig. 3A). To identify the markers and cell types driving these differences, we focused on the four markers with the highest PCA loadings, which contribute most strongly to the observed variation.

In the spleen, we found that monocytes expressing PD-L1 (p= 0.02), CD40 (p= 0.01), and CD70 (p= < 0.0001), as well as neutrophils expressing TIM-4 (p= 0.01), showed the greatest contribution to the separation between groups. In the lungs, macrophages expressing CD40 (p= 0.002) and CD64 (p= 0.04), along with neutrophils expressing CD80 (p= 0.005), were most distinct. In the liver, macrophages expressing CD40 (p= 0.001) and neutrophils expressing CD70 (p= 0.01) were the primary contributors (Fig. 3B).

Notably, the spleen displayed a more regulatory profile following IV immunization, characterized by decreased expression of activation markers CD40 and CD70, as well as the immune checkpoint marker PD-L1 (Fig. 3B). In contrast, in the lungs, IV immunization led to increased expression of CD64 on lung macrophages compared to ID immunization, suggesting enhanced activation and infiltration of monocyte-derived macrophages (Fig. 3B). In the liver, IV immunization led to upregulation of pro-

inflammatory markers CD70, CD40, and CD80, suggesting a shift toward a more inflammatory phenotype relative to ID immunization (Fig. 3B).

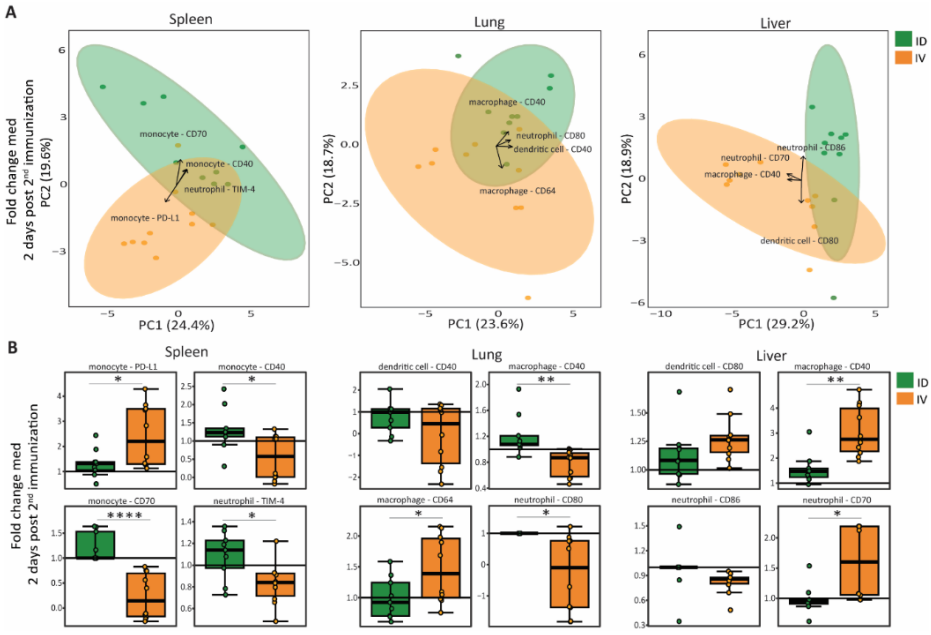

Figure 3. Activation of myeloid cells after intradermal (ID) and intravenous (IV) GA2 SPZ immunization. (A) Principal Component Analysis (PCA) plot of different markers on B-cells, neutrophils, macrophages, dendritic cells and monocytes after ID (green) of IV (orange) GA2 SPZ immunization in the spleen, lung and liver. MFI fold change relative to medium immunization, 2 days after the 2nd immunization. Markers and cell types responsible for the four highest loadings shown in the figure (**B)** Box plot of the markers and cell types responsible for the four highest loadings per organ between IV (orange) and ID (green) GA2 SPZ immunization. MFI fold change relative to medium, 2 days post 2nd immunization. ID immunization n=9 per group, IV immunization n=10 per group divided over 2 independent experiments. All conditions were *in vitro* restimulated with LA-GAP SPZ. Statistical significance between groups was assessed by an independent t-test. *p<0.05, **p<0.005, ***p<0.0005, and ****p<0.0001.

Distribution of immune cells in the skin and skin-draining lymph node

In an attempt to trace the source of the observed myeloid alteration, we examined the distribution of immune cells in the skin and skin-draining lymph node (skin dLN) after ID immunization. Two days after the second ID immunization, we observed an early increase in total number of immune cells in the skin after both SGE (p = 0.0006) and GA2 SPZ (p = 0.003) immunization, which normalized rapidly at 7 days after 2nd immunization (Fig. 4A). In the skin dLN we observed an increase in the total number of

immune cells at the early time point of 2 days after 2nd immunization with SGE (p = 0.0002) or GA2 SPZ (p = <0.0001), which remained stable at the later 7 days after 2nd immunization time point (Fig. 4B). This suggests that APC cells from the skin along with circulating B and T cells, migrate to the skin dLN within 2 days where antigen presentation and subsequent B and T cell activation occurs.

When we investigated the overall kinetics of immune cell distribution in the skin and skin dLN 2 days after 2nd ID immunization, we observed an increase in the percentage of eosinophils in SGE compared with medium (p = 0.02) and in SGE compared with GA2 SPZ (p = 0.009) immunization. At 7 days after 2nd immunization, we found an increase in the percentage of eosinophils after SGE (p = 0.06) and GA2 SPZ (p = 0.04) immunization. Additionally, we observed an increase in the percentage $CD3^+$ T cells after GA2 SPZ (p = 0.04) immunization (Fig. 4C). Interestingly, in the skin dLN we observed a striking increase in B-cells after GA2 SPZ administration (p = <0.0001) and SGE (p = 0.001) 2 days after 2nd immunization, but a lower percentage $CD3^+$ T cells after SGE (p = <0.0001) and GA2 SPZ (p = <0.0001) immunization (Fig. 4D). However, the total number of $CD3^+$ T cells after SGE (mean 408.10^4) and GA2 SPZ (366.10^4) immunization was slightly higher than medium (232.10^4) immunization (Sup Fig. 5A). Overall we found in the skin and skin dLN an increase in total number of monocytes, dendritic cells, macrophages, $CD3^+$ T cells and B-cells 2 days after 2nd GA2 SPZ immunization and SGE compared with medium (Sup Fig. 5A).

Next, we investigated the expression of activation and regulatory markers on myeloid cells in the skin and skin dLN 2 days after 2nd GA2 SPZ immunization compared with 2 days after 2nd medium immunization. Here we observed, next to an increase in activation marker CD64 and CD70 on monocytes and neutrophils, a striking decrease in expression of activation marker CD86 on dendritic cells, macrophages, monocytes and neutrophils (Fig. 4E+G). Compared to SGE immunization, GA2 SPZ immunization led to the upregulation of regulatory marker PD-L1 on dendritic cells (p = 0.09) and macrophages (p = 0.06) in the skin dLN (Fig. 4F+H). Last, in the skin, T cell activation appeared overall comparable between GA2 SPZ and SGE but in the skin dLN the activation of T cells after GA2 SPZ immunization seems slightly downregulated compared with SGE immunization for most activation markers (Sup Fig. 6A). In line with previous findings, we observed a decrease over time in the percentage of $IFNy^+$ $CD8^+$ T cells in the skin dLN (3.3%) [13], suggesting migration of these cells to other organs. This effect appeared to be specific to SPZ restimulation and was not observed following PMA/Iono restimulation (Sup Fig. 6B+C+D).

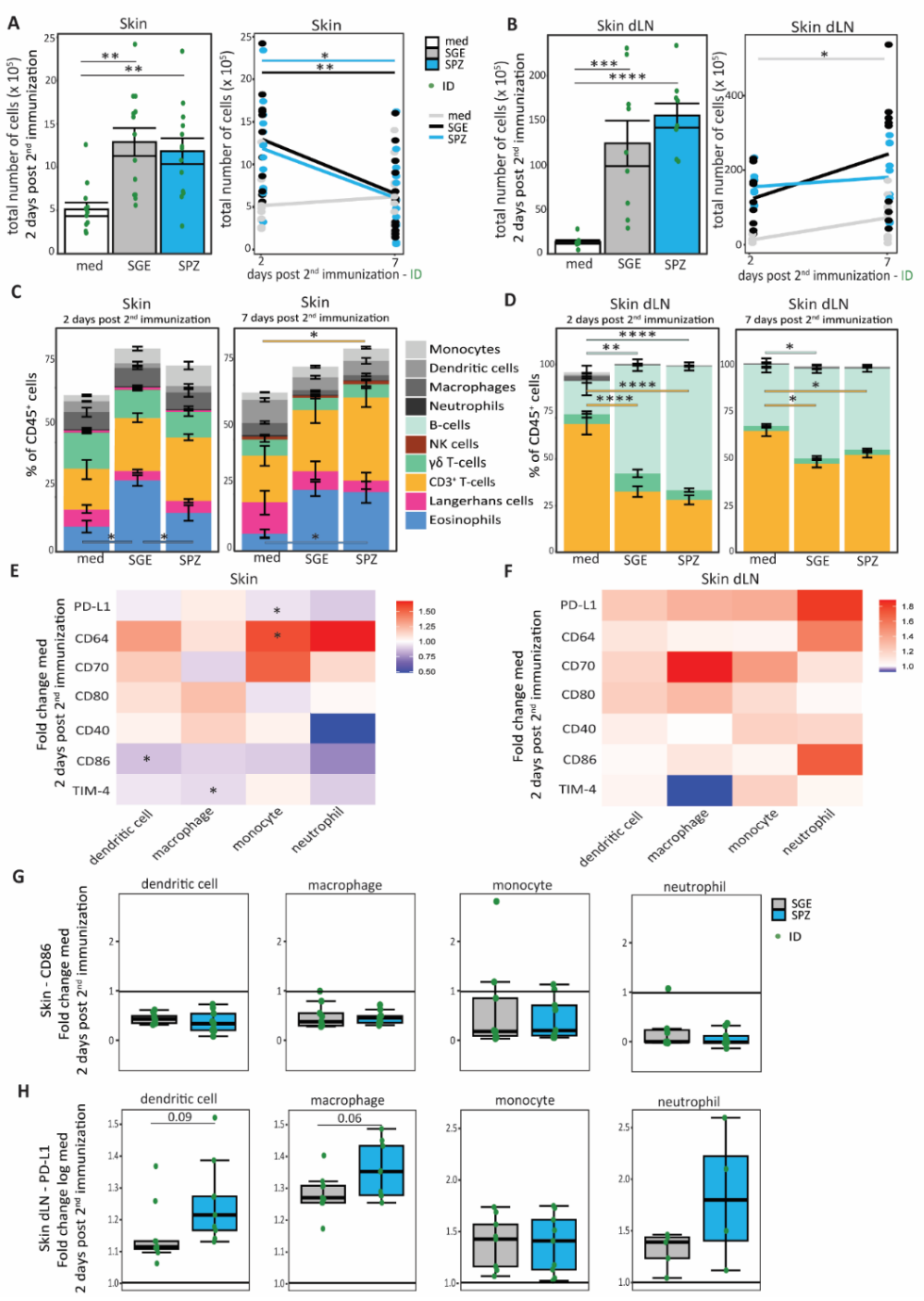

Figure 4. Cell distribution and myeloid activation in the skin and skin-draining lymph node (dLN). (A+B) The total number of immune cells in the skin (**A**) or skin dLN (**B**) *ex vivo*, after

medium (white), SGE (grey) or GA2 SPZ (blue) ID (green dots) immunization at 2 days or 7 days after 2nd immunization. (**C+D)** cell distribution in the skin (**C**) and skin dLN (**D**) after medium, SGE or GA2 SPZ immunization at 2 days or 7 days after 2nd immunization followed by *in vitro* restimulation with LA-GAP SPZ. (**E+F)** Heatmap of fold change relative to medium expression of different markers on myeloid cells for the skin (**E**) and skin dLN (**F**) 2 days after 2nd immunization followed by *in vitro* restimulation with LA-GAP SPZ. (**G)** Expression of CD86 in the skin on B-cells, dendritic cells, macrophages, monocytes and neutrophils after SGE (grey) or GA2 SPZ (blue) ID (green dots) immunization after *in vitro* restimulation with LA-GAP SPZ. (**H)** Expression of PD-L1 in the skin dLN on B-cells, dendritic cells, macrophages, monocytes and neutrophils after SGE (grey) or GA2 SPZ (blue) ID (green dots) immunization after *in vitro* restimulation with LA-GAP SPZ. Skin n=9-13 mice per group, skin dLN n=9 mice per group divided over 2 or 3 independent experiments. Statistical significance between groups was assessed by one-way ANOVA with multiple comparisons or an independent t-test. *p<0.05, **p<0.005, ***p<0.0005, and ****p<0.0001.

Overall, we observed an increase in the number of immune cells in both the skin and skin dLN, but an impressive decrease of activation marker CD86 on myeloid cells in the skin after GA2 SPZ immunization which also occurs after SGE immunization. However, GA2 SPZ immunization specifically led to the upregulation of regulatory marker PD-L1 on dendritic cells and macrophages in the skin dLN, suggesting the induction of a regulatory phenotype after ID GA2 SPZ immunization. This regulatory profile was not seen after SGE immunization and may impair the antigen-presenting capacity of dendritic cells and macrophages as they migrate from the skin dLN to other malaria-infected organs, potentially influencing the quality and magnitude of the systemic T-cell response (Fig. 5).

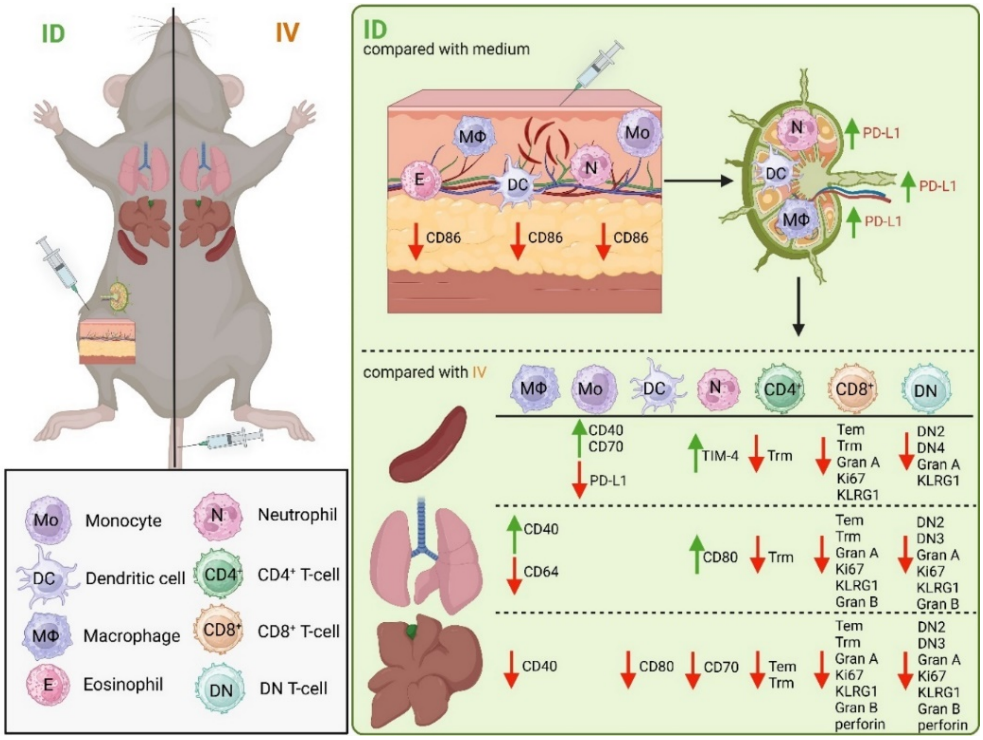

Figure 5. Summary. Immune responses after two immunizations with late arresting genetically attenuated parasite sporozoite (GA2 SPZ) in the skin, skin-draining lymph node, spleen, lungs and liver. Skin and skin draining lymph node GA2 SPZ intradermal immunization (ID, green) compared with medium ID immunization and spleen, lungs and liver GA2 SPZ ID compared with GA2 SPZ intravenous immunization (IV, orange).

Discussion

In summary, we compared the immune responses in the spleen, lung and liver after GA2 SPZ ID or IV immunization in a *Plasmodium berghei (Pb)* rodent malaria model to unravel the potential mechanisms underlying decreased protection of ID-immunized mice. Overall, our findings revealed a lower number of $CD8^+$ Trm cells and reduced activation of $CD8^+$ T cells and DN T cells after ID immunization compared with IV immunization, corroborating prior findings in the *Py* rodent malaria model [24]. In the skin, skin dLN and the liver we identified a large population of myeloid cells with a predominantly regulatory phenotype following ID GA2 SPZ immunization. These cells exhibited decreased CD86 expression in the skin and increased PD-L1 expression in the skin dLN. These results suggest that myeloid cells in the skin and skin dLN orchestrate a regulatory immune response resulting in a lower number of $CD8^+$ Trm cells and

diminished T cell activation in the spleen, lungs and liver after ID GA2 SPZ immunization as compared to IV immunization.

Our findings in mouse models may provide insight into why ID-administered whole SPZ vaccines are less effective at inducing protective immunity in humans. First, it has been shown that SPZ injected intradermally by needle are 3-fold less efficient in migrating and infecting mouse livers compared to mosquito-inoculated SPZ. Previously we suggested that this is a consequence of the changes in the dermal tissue morphology caused by the injection of larger volumes via needles, in contrast to the small volume saliva inoculation by mosquitoes [25]. Second, recent findings demonstrate that some SPZ remaining in the skin after ID immunization migrate to the skin dLN, where they may contribute to the induction of regulatory responses, characterized by PD-L1 expression on myeloid cells. These myeloid cells may, in turn, orchestrate the suppression of T cell activation, specifically to a reduction of $CD8^+$ Trm cells as well as decreased expression of Granzyme B and perforin. Previously, we have investigated the responses of human monocyte-derived macrophages when stimulated with SPZ and observed a similar regulatory phenotype. Similarly, we have shown that *in vitro* human dermal myeloid cells showed an increase in PD-L1 expression following exposure to SPZ [26]. Altogether these findings support our belief that the mechanisms observed in the *Pb* rodent model may be translatable to humans.

While investigating the myeloid activation in the skin we further observed a decrease in CD86 and TIM-4 expression, which suggests reduced T cell activation [27]. However, the increased expression of CD64 and CD70 points to a different, non-traditional pathway of T cell stimulation, possibly involving CD70 on myeloid cells and CD27 on T cells, which needs further study [28, 29]. In the skin dLN, we primarily observed increased PD-L1 expression, indicating a regulatory phenotype [30]. In the liver, we found decreased expression of activation markers CD40, CD70 and CD80 on myeloid cells after ID GA2 SPZ immunization compared with IV immunization. This suggests that regulatory immune activity in the skin dLN may modulate hepatic immune responses. Notably, dendritic cells, key players in T cell activation [31, 32], along with the expression of perforin on $CD8^+$ and DN T cells, were only affected in the liver after ID GA2 SPZ immunization. Together, these findings indicate that myeloid cell activity and T cell priming in the skin and dLN can shape downstream immune responses in the liver.

By passing through the skin, SPZ undergoes a “filtering” process allowing only viable and motile SPZ to enter the bloodstream. This filtering effect does not occur during IV

administration, where SPZ bypass the skin and its filtering mechanism, allowing also less motile or less viable SPZ to enter the bloodstream [25, 33]. By administering IV instead of ID, the skin and skin dLN will be passed, allowing "unfiltered" SPZ to enter the lungs. Consequently, a larger number of less motile and viable SPZ may become trapped in the lungs following IV immunization which could lead to more localized immune activation in the lungs [20]. Interestingly, although SPZ from ID immunization still travel through the lungs, we did not observe the presence of $CD8^+$ Trm cells in this organ. Furthermore, we saw increased Granzyme B expression in $CD8^+$ T cells and DN T cells following IV immunization but not after ID immunization, indicating lower activation in the lungs after ID immunization compared with IV immunization.

ID immunization is considered technically easier to perform than IV immunization [34]. Currently, several vaccines, including those for tuberculosis, influenza, and rabies, are administered through ID injection. These vaccines have been shown to be more effective when delivered at reduced doses [35-39]. For humans, the recommended volume for ID immunization typically ranges between 50 and 100 µL (NIH). In mice, the standard volume ranges from 10 to 50 µL (IACUC guideline), but recent studies suggest that whole SPZ ultra-low volumes as small as of 2.5 µL are more effective as they facilitate migration of SPZ out of the skin injection site [40, 41]. Reducing the volume of the vaccine administered may thus enhance the efficacy of ID GA2 SPZ vaccinations, changing the ratio of trapped versus migratory SPZ. This may result in a lower regulatory immune response and improve T cell activation. Additionally, if more SPZ exit the skin, a larger number will likely infect hepatocytes and develop into late liver schizonts, which is essential for generating effective protection after GA2 immunization [5]. Consequently, a lower dose for GA2 SPZ ID administration could lead to a more effective, easier-to-administer, and cost-effective vaccine.

In conclusion, we compared the immune response in the spleen, lungs and liver after GA2 SPZ ID and IV immunization and our findings revealed decreased T cell differentiation and activation after ID immunization. Additionally, upon examining the skin and skin dLN we observed a regulatory myeloid phenotype. These observations suggest that the regulatory myeloid cells in the skin and skin dLN influence the T cell differentiation and activation in the spleen, lungs and liver. These findings warrant further investigation to examine their impact on vaccine efficacy and to assess whether protection following GA2 SPZ ID immunization can be strengthened.

Acknowledgment

We would like to thank the flow cytometry facility of the LUMC.

References

1. Roozen GVT, van Schuijlenburg R, Hensen ADO, Koopman JPR, Lamers OAC, Geurten FJA, Sijtsma JC, Baalbergen E, Janse JJ, Chevalley-Maurel S, Naar CM, Bezemer S, Kroeze H, van de Stadt HJF, de Visser B, Meij P, Tihaya MS, Colstrup E, Iliopoulou E, de Bes-Roeleveld HM, Wessels E, van der Stoep M, Janse CJ, Murugan R, Franke-Fayard BMD, Roestenberg M. Single immunization with genetically attenuated PfΔmei2 (GA2) parasites by mosquito bite in controlled human malaria infection: a placebo-controlled randomized trial. Nat Med. 2025;31(1):218-22. Epub 20250103. doi: 10.1038/s41591-024-03347-2. PubMed PMID: 39753962; PMCID: PMC11750698.
2. Franke-Fayard B, Marin-Mogollon C, Geurten FJA, Chevalley-Maurel S, Ramesar J, Kroeze H, Baalbergen E, Wessels E, Baron L, Soulard V, Martinson T, Aleshnick M, Huijs ATG, Subudhi AK, Miyazaki Y, Othman AS, Kolli SK, Lamers OAC, Roques M, Stanway RR, Murphy SC, Foquet L, Moita D, Mendes AM, Prudencio M, Dechering KJ, Heussler VT, Pain A, Wilder BK, Roestenberg M, Janse CJ. Creation and preclinical evaluation of genetically attenuated malaria parasites arresting growth late in the liver. NPJ Vaccines. 2022;7(1):139. Epub 20221104. doi: 10.1038/s41541-022-00558-x. PubMed PMID: 36333336; PMCID: PMC9636417.
3. Prudencio M, Rodriguez A, Mota MM. The silent path to thousands of merozoites: the Plasmodium liver stage. Nat Rev Microbiol. 2006;4(11):849-56. doi: 10.1038/nrmicro1529. PubMed PMID: 17041632.
4. Beeson JG, Drew DR, Boyle MJ, Feng G, Fowkes FJ, Richards JS. Merozoite surface proteins in red blood cell invasion, immunity and vaccines against malaria. FEMS Microbiol Rev. 2016;40(3):343-72. Epub 20160131. doi: 10.1093/femsre/fuw001. PubMed PMID: 26833236; PMCID: PMC4852283.
5. Lamers OAC, Franke-Fayard BMD, Koopman JPR, Roozen GVT, Janse JJ, Chevalley-Maurel SC, Geurten FJA, de Bes-Roeleveld HM, Iliopoulou E, Colstrup E, Wessels E, van Gemert GJ, van de Vegte-Bolmer M, Graumans W, Stoter TR, Mordmuller BG, Houlder EL, Bousema T, Murugan R, McCall MBB, Janse CJ, Roestenberg M. Safety and Efficacy of Immunization with a Late-Liver-Stage Attenuated Malaria Parasite. N Engl J Med. 2024;391(20):1913-23. doi: 10.1056/NEJMoa2313892. PubMed PMID: 39565990.
6. Fernandez-Ruiz D, Ng WY, Holz LE, Ma JZ, Zaid A, Wong YC, Lau LS, Mollard V, Cozijnsen A, Collins N, Li J, Davey GM, Kato Y, Devi S, Skandari R, Pauley M, Manton JH, Godfrey DI, Braun A, Tay SS, Tan PS, Bowen DG, Koch-Nolte F, Rissiek B, Carbone FR, Crabb BS, Lahoud M, Cockburn IA, Mueller SN, Bertolino

P, McFadden GI, Caminschi I, Heath WR. Liver-Resident Memory CD8(+) T Cells Form a Front-Line Defense against Malaria Liver-Stage Infection. Immunity. 2016;45(4):889-902. Epub 20160927. doi: 10.1016/j.immuni.2016.08.011. PubMed PMID: 27692609.

7. Zhu C, Jiao S, Xu W. CD8(+) Trms against malaria liver-stage: prospects and challenges. Front Immunol. 2024;15:1344941. Epub 20240122. doi: 10.3389/fimmu.2024.1344941. PubMed PMID: 38318178; PMCID: PMC10839007.
8. Doolan DL, Hoffman SL. The complexity of protective immunity against liver-stage malaria. J Immunol. 2000;165(3):1453-62. doi: 10.4049/jimmunol.165.3.1453. PubMed PMID: 10903750.
9. Lefebvre MN, Harty JT. You Shall Not Pass: Memory CD8 T Cells in Liver-Stage Malaria. Trends Parasitol. 2020;36(2):147-57. Epub 20191213. doi: 10.1016/j.pt.2019.11.004. PubMed PMID: 31843536; PMCID: PMC6937381.
10. Overstreet MG, Cockburn IA, Chen YC, Zavala F. Protective CD8 T cells against Plasmodium liver stages: immunobiology of an 'unnatural' immune response. Immunol Rev. 2008;225:272-83. doi: 10.1111/j.1600-065X.2008.00671.x. PubMed PMID: 18837788; PMCID: PMC2597001.
11. Corradin G, Levitskaya J. Priming of CD8(+) T Cell Responses to Liver Stage Malaria Parasite Antigens. Front Immunol. 2014;5:527. Epub 20141105. doi: 10.3389/fimmu.2014.00527. PubMed PMID: 25414698; PMCID: PMC4220712.
12. Hassert M, Arumugam S, Harty JT. Memory CD8+ T cell-mediated protection against liver-stage malaria. Immunol Rev. 2023;316(1):84-103. Epub 20230404. doi: 10.1111/imr.13202. PubMed PMID: 37014087; PMCID: PMC10524177.
13. Chakravarty S, Cockburn IA, Kuk S, Overstreet MG, Sacci JB, Zavala F. CD8+ T lymphocytes protective against malaria liver stages are primed in skin-draining lymph nodes. Nat Med. 2007;13(9):1035-41. Epub 20070819. doi: 10.1038/nm1628. PubMed PMID: 17704784.
14. Radtke AJ, Kastenmuller W, Espinosa DA, Gerner MY, Tse SW, Sinnis P, Germain RN, Zavala FP, Cockburn IA. Lymph-node resident CD8alpha+ dendritic cells capture antigens from migratory malaria sporozoites and induce CD8+ T cell responses. PLoS Pathog. 2015;11(2):e1004637. Epub 20150206. doi: 10.1371/journal.ppat.1004637. PubMed PMID: 25658939; PMCID: PMC4450069.
15. Yap XZ, Lundie RJ, Beeson JG, O'Keeffe M. Dendritic Cell Responses and Function in Malaria. Front Immunol. 2019;10:357. Epub 20190304. doi: 10.3389/fimmu.2019.00357. PubMed PMID: 30886619; PMCID: PMC6409297.

16. Holz LE, Prier JE, Freestone D, Steiner TM, English K, Johnson DN, Mollard V, Cozijnsen A, Davey GM, Godfrey DI, Yui K, Mackay LK, Lahoud MH, Caminschi I, McFadden GI, Bertolino P, Fernandez-Ruiz D, Heath WR. CD8(+) T Cell Activation Leads to Constitutive Formation of Liver Tissue-Resident Memory T Cells that Seed a Large and Flexible Niche in the Liver. Cell Rep. 2018;25(1):68-79 e4. doi: 10.1016/j.celrep.2018.08.094. PubMed PMID: 30282039.
17. Sinnis P, Zavala F. The skin: where malaria infection and the host immune response begin. Semin Immunopathol. 2012;34(6):787-92. Epub 20121002. doi: 10.1007/s00281-012-0345-5. PubMed PMID: 23053392; PMCID: PMC3934925.
18. Gueirard P, Tavares J, Thiberge S, Bernex F, Ishino T, Milon G, Franke-Fayard B, Janse CJ, Menard R, Amino R. Development of the malaria parasite in the skin of the mammalian host. Proc Natl Acad Sci U S A. 2010;107(43):18640-5. Epub 20101004. doi: 10.1073/pnas.1009346107. PubMed PMID: 20921402; PMCID: PMC2972976.
19. Menard R. The journey of the malaria sporozoite through its hosts: two parasite proteins lead the way. Microbes Infect. 2000;2(6):633-42. doi: 10.1016/s1286-4579(00)00362-2. PubMed PMID: 10884614.
20. van Schuijlenburg R, Naar CM, van der Wees S, Chevalley-Maurel SC, Duszenko N, de Bes-Roeleveld HM, Iliopoulou E, Houlder EL, Geurten FJA, Baalbergen E, Roestenberg M, Franke-Fayard B. Early Activation of Lung CD8(+) T Cells After Immunization with Live Plasmodium berghei Malaria Sporozoites. Pathog Immun. 2025;10(2):46-68. Epub 20250304. doi: 10.20411/pai.v10i2.794. PubMed PMID: 40062354; PMCID: PMC11888604.
21. Obeid M, Franetich JF, Lorthiois A, Gego A, Gruner AC, Tefit M, Boucheix C, Snounou G, Mazier D. Skin-draining lymph node priming is sufficient to induce sterile immunity against pre-erythrocytic malaria. EMBO Mol Med. 2013;5(2):250-63. Epub 20121219. doi: 10.1002/emmm.201201677. PubMed PMID: 23255300; PMCID: PMC3569641.
22. Bastiaens GJH, van Meer MPA, Scholzen A, Obiero JM, Vatanshenassan M, van Grinsven T, Sim BKL, Billingsley PF, James ER, Gunasekera A, Bijker EM, van Gemert GJ, van de Vegte-Bolmer M, Graumans W, Hermsen CC, de Mast Q, van der Ven A, Hoffman SL, Sauerwein RW. Safety, Immunogenicity, and Protective Efficacy of Intradermal Immunization with Aseptic, Purified, Cryopreserved Plasmodium falciparum Sporozoites in Volunteers Under Chloroquine Prophylaxis: A Randomized Controlled Trial. Am J Trop Med Hyg.

2016;94(3):663-73. Epub 20151228. doi: 10.4269/ajtmh.15-0621. PubMed PMID: 26711509; PMCID: PMC4775905.

23. Parmar R, Patel H, Yadav N, Patidar M, Tyagi RK, Dalai SK. Route of administration of attenuated sporozoites is instrumental in rendering immunity against Plasmodia infection. Vaccine. 2016;34(28):3229-34. Epub 20160506. doi: 10.1016/j.vaccine.2016.04.095. PubMed PMID: 27160038.
24. Haeberlein S, Chevalley-Maurel S, Ozir-Fazalalikhan A, Koppejan H, Winkel BMF, Ramesar J, Khan SM, Sauerwein RW, Roestenberg M, Janse CJ, Smits HH, Franke-Fayard B. Protective immunity differs between routes of administration of attenuated malaria parasites independent of parasite liver load. Sci Rep. 2017;7(1):10372. Epub 20170904. doi: 10.1038/s41598-017-10480-1. PubMed PMID: 28871201; PMCID: PMC5583236.
25. de Korne CM, Winkel BMF, van Oosterom MN, Chevalley-Maurel S, Houwing HM, Sijtsma JC, Azargoshasb S, Baalbergen E, Franke-Fayard BMD, van Leeuwen FWB, Roestenberg M. Clustering and Erratic Movement Patterns of Syringe-Injected versus Mosquito-Inoculated Malaria Sporozoites Underlie Decreased Infectivity. mSphere. 2021;6(2). Epub 20210407. doi: 10.1128/mSphere.00218-21. PubMed PMID: 33827910; PMCID: PMC8546700.
26. Winkel BMF, Pelgrom LR, van Schuijlenburg R, Baalbergen E, Ganesh MS, Gerritsma H, de Korne CM, Duszenko N, Langenberg MCC, Chevalley-Maurel SC, Smits HH, de Jong EC, Everts B, Franke-Fayard B, Roestenberg M. Plasmodium sporozoites induce regulatory macrophages. PLoS Pathog. 2020;16(9):e1008799. Epub 20200908. doi: 10.1371/journal.ppat.1008799. PubMed PMID: 32898164; PMCID: PMC7500643.
27. Rodriguez-Manzanet R, Meyers JH, Balasubramanian S, Slavik J, Kassam N, Dardalhon V, Greenfield EA, Anderson AC, Sobel RA, Hafler DA, Strom TB, Kuchroo VK. TIM-4 expressed on APCs induces T cell expansion and survival. J Immunol. 2008;180(7):4706-13. doi: 10.4049/jimmunol.180.7.4706. PubMed PMID: 18354194; PMCID: PMC2948965.
28. Lutfi F, Wu L, Sunshine S, Cao X. Targeting the CD27-CD70 Pathway to Improve Outcomes in Both Checkpoint Immunotherapy and Allogeneic Hematopoietic Cell Transplantation. Front Immunol. 2021;12:715909. Epub 20210922. doi: 10.3389/fimmu.2021.715909. PubMed PMID: 34630390; PMCID: PMC8493876.
29. Denoeud J, Moser M. Role of CD27/CD70 pathway of activation in immunity and tolerance. J Leukoc Biol. 2011;89(2):195-203. Epub 20100810. doi: 10.1189/jlb.0610351. PubMed PMID: 20699361.

30. Peng Q, Qiu X, Zhang Z, Zhang S, Zhang Y, Liang Y, Guo J, Peng H, Chen M, Fu YX, Tang H. PD-L1 on dendritic cells attenuates T cell activation and regulates response to immune checkpoint blockade. Nat Commun. 2020;11(1):4835. Epub 20200924. doi: 10.1038/s41467-020-18570-x. PubMed PMID: 32973173; PMCID: PMC7518441.
31. Theisen D, Murphy K. The role of cDC1s in vivo: CD8 T cell priming through cross-presentation. F1000Res. 2017;6:98. Epub 20170201. doi: 10.12688/f1000research.9997.1. PubMed PMID: 28184299; PMCID: PMC5288679.
32. Zinkernagel RM. On the Role of Dendritic Cells Versus Other Cells in Inducing Protective CD8+ T Cell Responses. Front Immunol. 2014;5:30. Epub 20140210. doi: 10.3389/fimmu.2014.00030. PubMed PMID: 24575091; PMCID: PMC3918652.
33. Yamauchi LM, Coppi A, Snounou G, Sinnis P. Plasmodium sporozoites trickle out of the injection site. Cell Microbiol. 2007;9(5):1215-22. Epub 20070109. doi: 10.1111/j.1462-5822.2006.00861.x. PubMed PMID: 17223931; PMCID: PMC1865575.
34. Hickling JK, Jones KR, Friede M, Zehrung D, Chen D, Kristensen D. Intradermal delivery of vaccines: potential benefits and current challenges. Bull World Health Organ. 2011;89(3):221-6. Epub 20110105. doi: 10.2471/BLT.10.079426. PubMed PMID: 21379418; PMCID: PMC3044245.
35. Lee S, Kim T, Seong KY, Yim SG, Lee WK, Kim S, Lee KO, Yang SY, Ryoo S. Microneedle-mediated intradermal delivery of Bacille Calmette-Guerin (BCG) vaccines for single-dose tuberculosis vaccination. Tuberculosis (Edinb). 2025;151:102608. Epub 20250116. doi: 10.1016/j.tube.2025.102608. PubMed PMID: 39832400.
36. Hung IFN, Yuen KY. Immunogenicity, safety and tolerability of intradermal influenza vaccines. Hum Vaccin Immunother. 2018;14(3):565-70. Epub 20170706. doi: 10.1080/21645515.2017.1328332. PubMed PMID: 28604266; PMCID: PMC5861844.
37. Gongal G, Sampath G. Introduction of intradermal rabies vaccination - A paradigm shift in improving post-exposure prophylaxis in Asia. Vaccine. 2019;37 Suppl 1:A94-A8. Epub 20180824. doi: 10.1016/j.vaccine.2018.08.034. PubMed PMID: 30150166.
38. Kim YC, Jarrahian C, Zehrung D, Mitragotri S, Prausnitz MR. Delivery systems for intradermal vaccination. Curr Top Microbiol Immunol. 2012;351:77-112. doi: 10.1007/82_2011_123. PubMed PMID: 21472533; PMCID: PMC3173582.

39. Saitoh A, Aizawa Y. Intradermal vaccination for infants and children. Hum Vaccin Immunother. 2016;12(9):2447-55. Epub 20160502. doi: 10.1080/21645515.2016.1176652. PubMed PMID: 27135736; PMCID: PMC5027705.

40. Watson FN, Shears MJ, Kalata AC, Duncombe CJ, Seilie AM, Chavtur C, Conrad E, Cruz Talavera I, Raappana A, Sather DN, Chakravarty S, Sim BKL, Hoffman SL, Tsuji M, Murphy SC. Ultra-low volume intradermal administration of radiation-attenuated sporozoites with the glycolipid adjuvant 7DW8-5 completely protects mice against malaria. Sci Rep. 2024;14(1):2881. Epub 20240204. doi: 10.1038/s41598-024-53118-9. PubMed PMID: 38311678; PMCID: PMC10838921.

41. Voza T, Kebaier C, Vanderberg JP. Intradermal immunization of mice with radiation-attenuated sporozoites of Plasmodium yoelii induces effective protective immunity. Malar J. 2010;9:362. Epub 20101215. doi: 10.1186/1475-2875-9-362. PubMed PMID: 21159170; PMCID: PMC3014973.

42. Fougere A, Jackson AP, Bechtsi DP, Braks JA, Annoura T, Fonager J, Spaccapelo R, Ramesar J, Chevalley-Maurel S, Klop O, van der Laan AM, Tanke HJ, Kocken CH, Pasini EM, Khan SM, Bohme U, van Ooij C, Otto TD, Janse CJ, Franke-Fayard B. Correction: Variant Exported Blood-Stage Proteins Encoded by Plasmodium Multigene Families Are Expressed in Liver Stages Where They Are Exported into the Parasitophorous Vacuole. PLoS Pathog. 2017;13(1):e1006128. Epub 20170117. doi: 10.1371/journal.ppat.1006128. PubMed PMID: 28095481; PMCID: PMC5240906.

43. Annoura T, Chevalley S, Janse CJ, Franke-Fayard B, Khan SM. Quantitative analysis of Plasmodium berghei liver stages by bioluminescence imaging. Methods Mol Biol. 2013;923:429-43. doi: 10.1007/978-1-62703-026-7_30. PubMed PMID: 22990796.

Supplementary

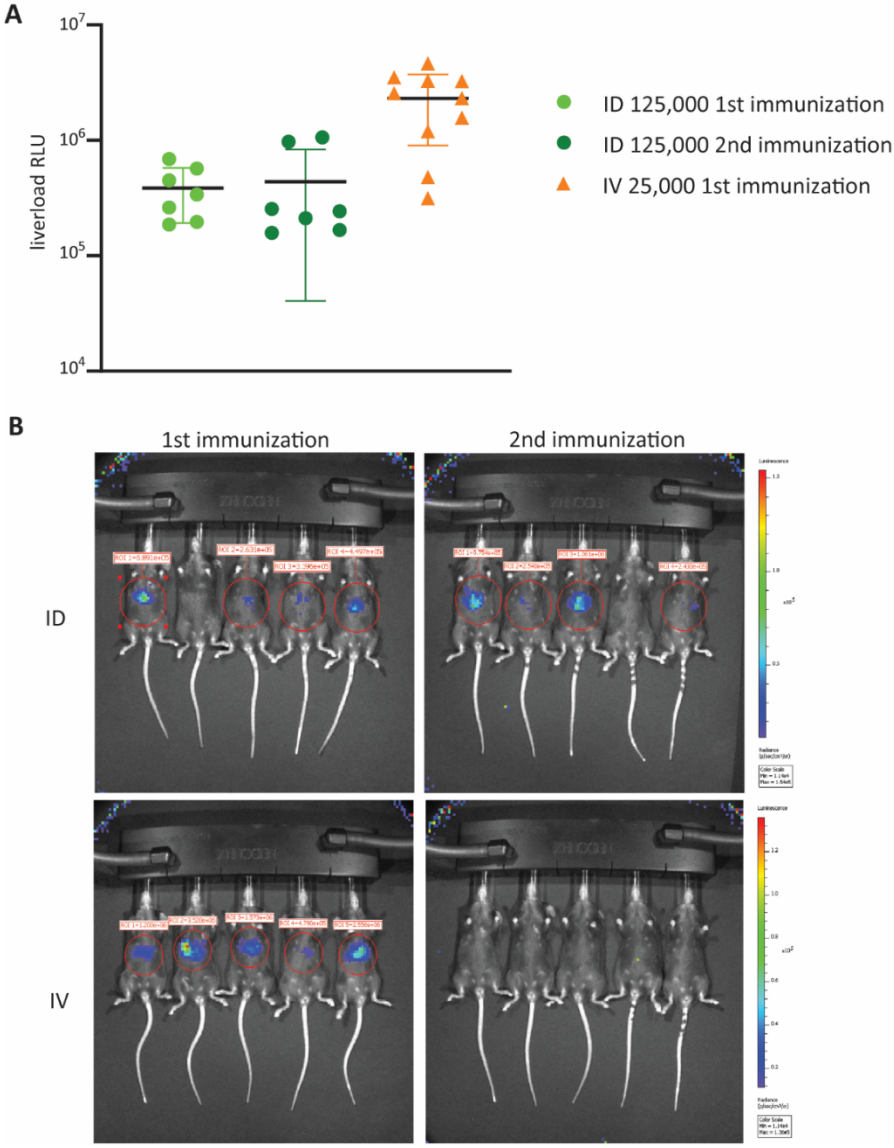

Supplementary figure 1. (A) Parasitic liver load 44 hours after ID (green) or IV (orange) administration measured by RLU. (**B)** Images of IVIS measurements of mice injected for the first or second time with GA2 SPZ via ID or IV immunization.

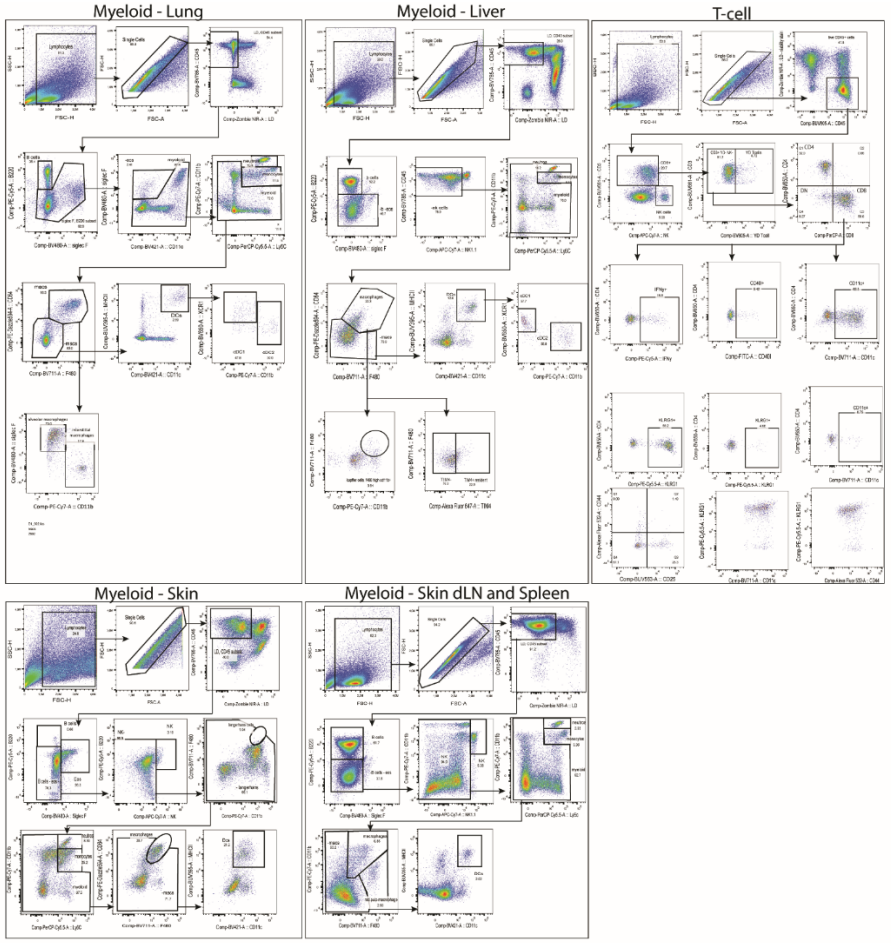

Supplementary figure 2. Gating strategy of myeloid cells for the lung, liver, skin, skin dLN and spleen. For the T cell gating same strategy has been used for all the organs.

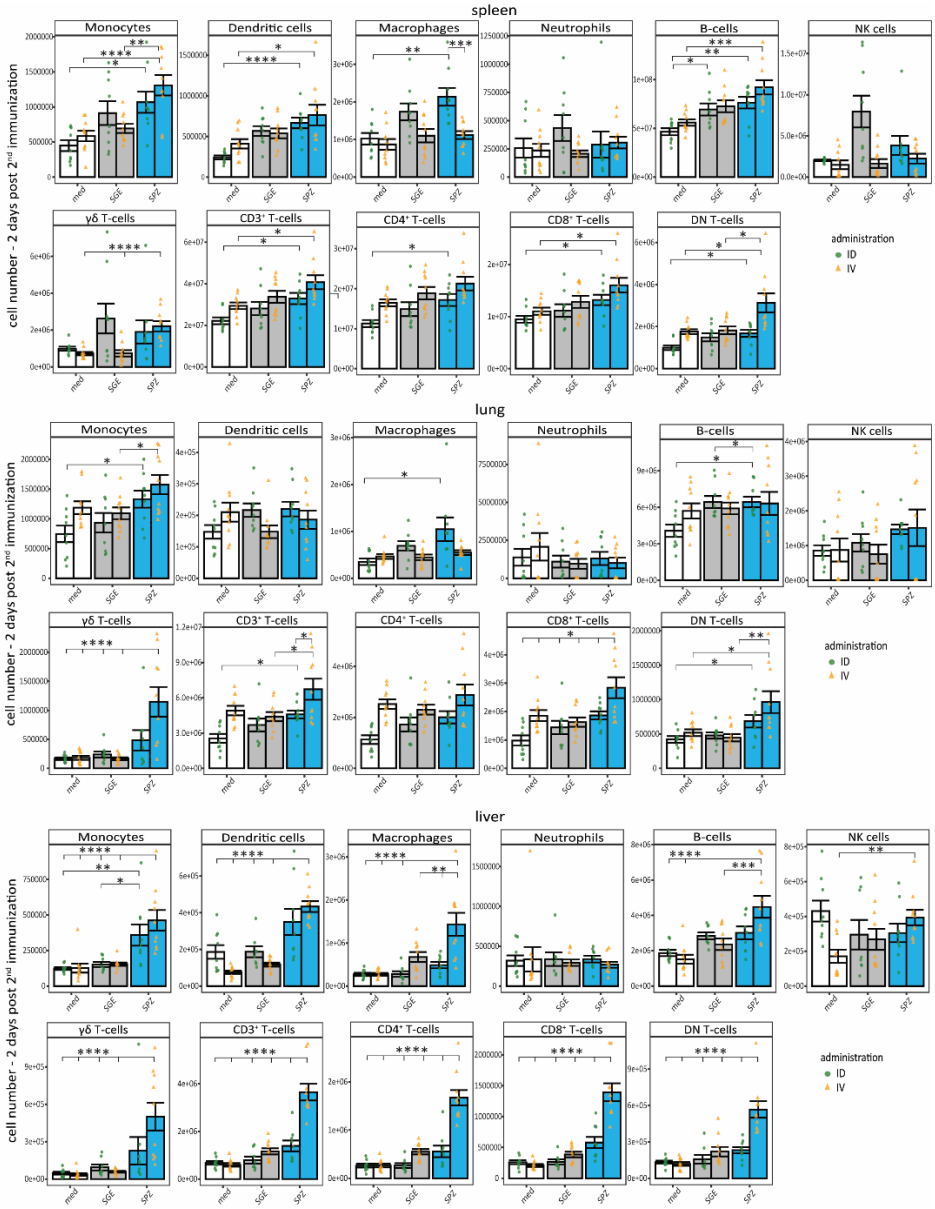

Supplementary figure 3. The absolute cell number of various immune cells in the spleen, lung and liver after medium (white), salivary gland extract (SGE) (grey) or GA2 sporozoite (SPZ) (blue) ID (green) or IV (orange) immunization. All conditions were *in vitro* restimulated with LA-GAP SPZ. ID immunization n=9 per group, IV immunization n=10 per group divided over 2 independent experiments. Statistical significance between groups was assessed by one-way ANOVA with multiple comparisons with Bonferroni correction. *p<0.05, **p<0.005, ***p<0.0005, and ****p<0.0001.

Supplementary figure 4. (**A**) Differences between expression of different markers on CD4$^+$ T cells in the spleen, lung and liver after ID (green) or IV (orange) GA2 SPZ immunization. Measured by fold change relative to medium. (**B**) Differences between expression of different markers on γδ T cells in the spleen, lung and liver after ID (green) or IV (orange) GA2 SPZ immunization. Measured by fold change log scale relative to medium. All conditions were *in vitro* restimulated with LA-GAP SPZ. ID immunization n=9 per group, IV immunization n=10 per group divided over 2 independent experiments. Statistical significance between groups was assessed by one-way ANOVA with multiple comparisons with Bonferroni correction. *p<0.05, **p<0.005, ***p<0.0005, and ****p<0.0001.

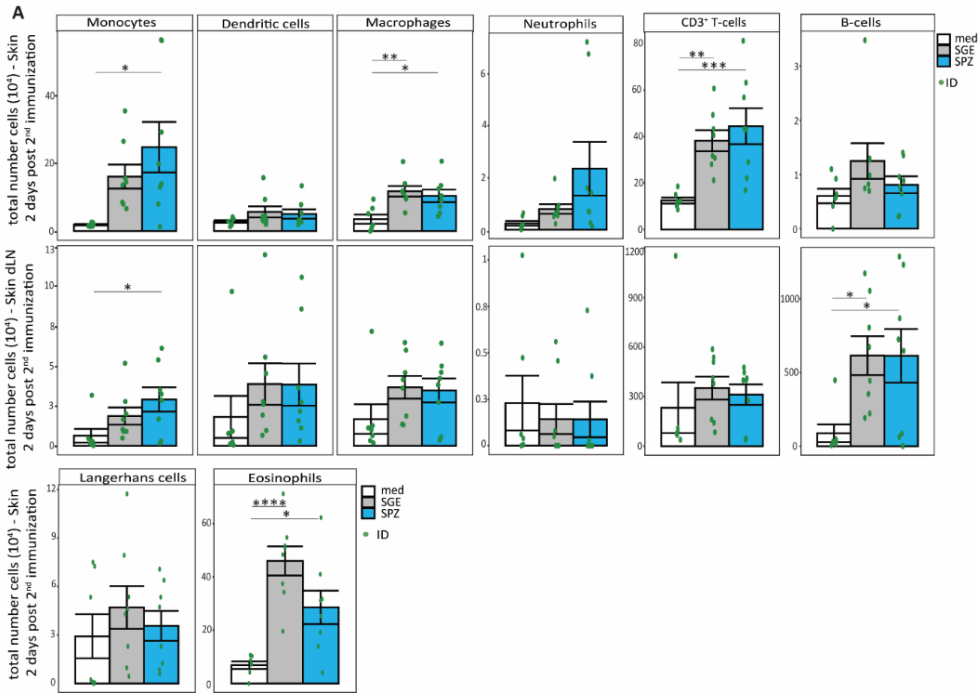

Supplementary figure 5. (A) The total number of monocytes, dendritic cells, macrophages, neutrophils CD3+ T cells and B cells in the skin and skin dLN, and Langerhans cells and eosinophils in the skin. Ex vivo counted 2 days after 2nd ID immunization with medium (white), SGE (grey) or GA2 SPZ (blue). Skin n=9-13 mice per group, skin dLN n=9 mice per group divided over 2 or 3 independent experiments. Statistical significance between groups was assessed by one-way ANOVA with multiple comparisons or an independent t-test. *p<0.05, **p<0.005, ***p<0.0005, and ****p<0.0001.

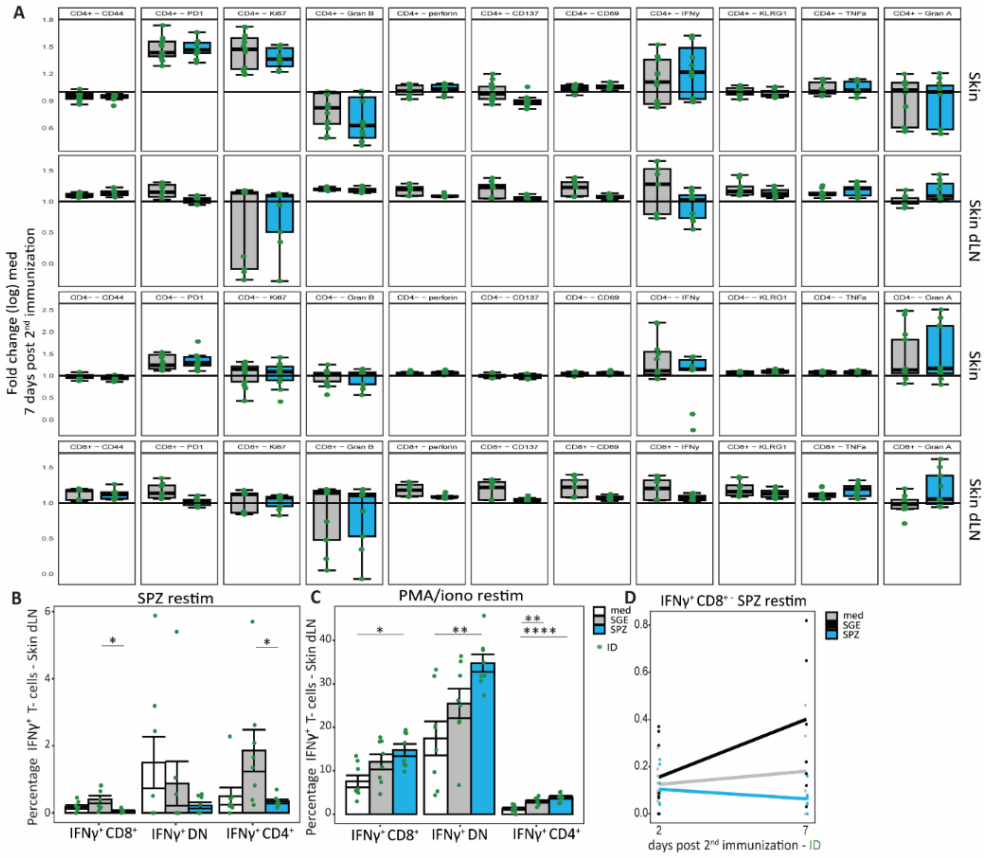

Supplementary figure 6. (A) Activation of $CD4^+$ and $CD4^-$ T cells in the skin and $CD4^+$ and $CD8^+$ T cells in the skin dLN. 7 days post 2nd immunization of SGE (grey) or GA2 SPZ (blue), measured by fold change relative to medium log scale. (**B)** Percentage of $IFN\gamma^+$ $CD8^+$, $CD4^+$ or DN T cells after SPZ (**B**) or PMA/Iono (**C**) restimulation 7 days after 2nd ID immunization. D. The amount of $IFN\gamma^+$ $CD8^+$ T cells over time measured by 2 days post 2nd GA2 SPZ immunization and 7 days post 2nd GA2 SPZ immunization. medium (grey), SGE (black) or GA2 SPZ (blue). All conditions were *in vitro* restimulated with LA-GAP SPZ. Skin n=9-13 mice per group, skin dLN n=9 mice per group divided over 2 or 3 independent experiments. Statistical significance between groups was assessed by one-way ANOVA with multiple comparisons or an independent t-test. *p<0.05, **p<0.005, ***p<0.0005, and ****p<0.0001.